AIAA SciTech Forum
9 - 13 January 2017, Grapevine, Texas
55th AIAA Aerospace Sciences Meeting

Estimation of Balance Uncertainty Using Direct Monte Carlo Simulation (DSMC) on a CPU-GPU architecture.

P M Bidgood[1]
CSIR, Brummeria, Pretoria, 0001, South Africa

The estimation of balance uncertainty using conventional satistical and error propagation methods has been found to be both approximate and laborious to the point of being untenable[1]. Direct Simulation by Monte Carlo (DSMC) has been shown to be an effective altenative[2]. The long simulation times of DSMC, when applied using conventional sequential codes, has been addressed by re-formulating the code to run on a multiple CPU-GPU, platform. Simulation times spanning minutes have replaced those spanning several hours. Application of uncertainty analysis using DSMC has led to an improvement in both balance calibration-quality and calibration-time, and promises to add understanding and insight not only to balance performance, calibration systems, and balance uncertainty, but also to an improved understanding of commonly quoted statistical data.

This paper extends the introductory paper presented in 2013[3] to provide an overview of the current CPU-GPU system[4]. Data obtained from a six component internal balance is used to show how the relatively large quantity of data generated using DSMC can be managed through the mechanism of data modeling. These models may be used to generate equivalent data related to balance loads as would be generated by a balance when performing a dead-weight roll-polar. This is considered to be not only an effective analysis approach, it also provides a practical link between data generated by a DSMC simulation and data that can be physically generated by a balance. Balance data from a roll-polar is used to show that balance uncertainties arising from the mathematical calibration model, the calibration-loading, and the balance itself, can be seperated and quantified. This leads to the recommendation that verification of correct balance installation and the determination of installed uncertainty be obtained by performing a dead-weight roll-polar. This provides confidence in the balance installation, balance uncertainty data, as well as minimisation of installation roll-offset error.

Nomenclature

Polar	=	used to specifically indicate a roll scan
%FS	=	% = percentage of full scale
PEs	=	Propagated Error (signal) - signal uncertainty propagated through a model of zero uncertainty.
PEm	=	Propagated Error (model) - zero uncertainty signal propagated through model uncertainty.
TPE	=	Total Propagated Error - signal uncertainty propagated through model uncertainty.
CSLu	=	Calibration System Loading uncertainty
DSMC	=	MCS = Direct Simulation by Monte Carlo or Monte Carlo Simulation
NF	=	Normal Force
PM	=	Pitching Moment
SF	=	Side Force
YM	=	Yawing Moment
DOE	=	Design of Experiment
MDOE	=	Modern Design of Experiment
TMISC	=	Total miscellaneous errors including thermal, hysteresis, loading and PEs.
MISC	=	Miscelaneous errors excluding load application errors
ANOVA	=	Analysis of Variance

[1]Balance specialist, ASC (Aeronautical Systems Competency),DPSS,CSIR, e-mail: pmbidgoo@csir.co.za

I. Introduction

The use of multiple regression statistics (ANOVA), to define the accuracy of an internal strain-gauged wind tunnel balance is known to provide only an approximate estimate. The absence of any relationship to the "true" values of the source data results in optimistic estimates of actual balance accuracy. If post-calibration confirmation points are obtained, the reported errors are a combination of balance error and errors in the application of the loads. The result is an exaggerated error which cannot be assigned to the balance alone. The accuracy of the calibration model itself is subject to balance-specific errors, load application errors (including alignment and dimensional errors), as well as regression errors. These are currently considered to be inseparable[5].

Numerous approaches to understanding and improving balance accuracy have been adopted. Such approaches include increased calibration data sets using automatic calibration machines, and Modern Design of Experiments (MDOE). However, in order to fully understand the underlying factors driving balance accuracy, the uncertainty of the loads applied during calibration and verification need to be known. Mathematical (statistical) modelling of the propagation of error through the balance calibration process has been shown[1] to be possible but un-tenable for general application. Similarly, a Monte Carlo Simulation (DSMC) approach was found [2] to require long computation times combined with the need to manage and evaluate relatively large volumes of data.

In 2014 it was demonstrated[4] that the parallel processing capability of a multiple Central Processing Unit (7 CPUs) combined with an array of Graphics Processor Units (2000+ GPUs) could be used to perform a Monte Carlo simulation with computational times which are not much different from those required to perform a single regression and statistical analysis. The large volume of data produced by DSMC remained.

The DSMC software referred to in this paper has only recently been completed in its current high-speed form. This paper presents some sample analysis results taken from a six-component balance, and provides some indication as to how the DSMC system can be utilized. The use of the trigonometric nature of the variation of a dead-weight load with roll angle is a practical physical reference for such investigations. The method requires only that the uncertainty in roll (angular uncertainty), and a single load magnitude (mass and gravity), be known in order to evaluate balance force measurement accuracy at a large number of off-calibration points. Evaluation of moment accuracy requires an additional moment arm (length) uncertainty value. Dead-weight roll polars are therfore used to examine DSMC data as well as to obtain balance data for verification purposes.

While statistical analysis requires the assumption of constant variance throughout the six-dimensional calibration space, this assumption is not required in DSMC. Results are therefore a function of a particular point in the calibration space; that is, results are a function of load magnitudes and load-combination. This presents a problem with respect to general reporting and the provision of understandable and useable data suitable for use by the end-user.

II. MCS Overview

The simulation process and its application are described by the author in Ref. 4. One perspective of the CPU-

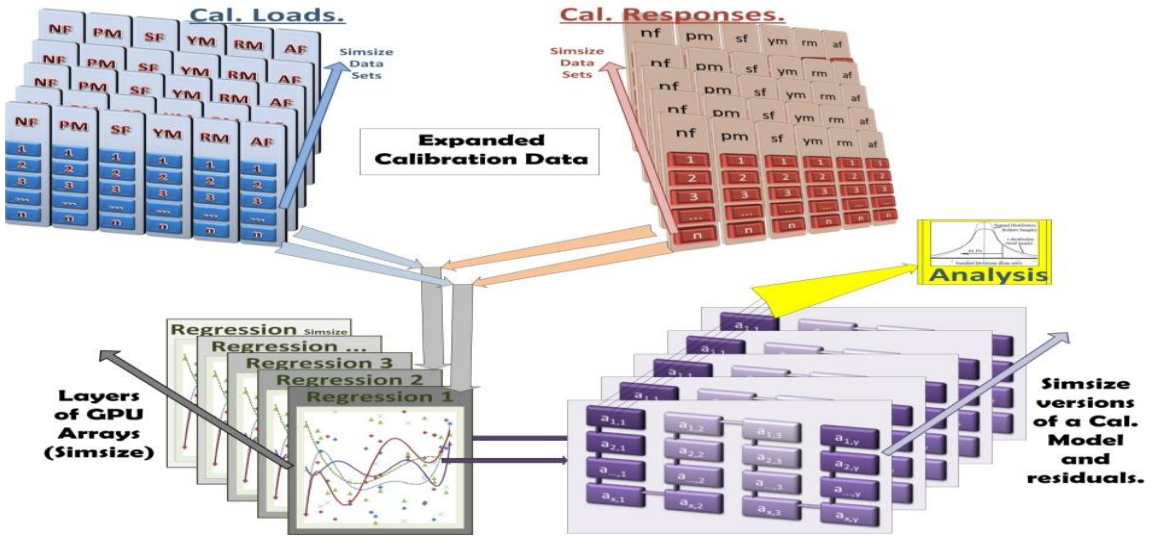

Figure 1. Parallel Regression Scheme. *The sheme is duplicated on a separate CPU for each component.*

GPU structure for MCS regressions is illustrated in Fig. 1. Input data is in the form of quantities that are chosen to be as fundamental as possible. Wherever possible, the fundamental uncertainties are derived from secondary standards. Any fundamental value is expanded into a large number of values which, *collectively*, is equivalent to a combination of the supplied value *and* it's uncertainty. Thereafter, random combinations of this data are selected to form numerous calibration data sets, which are then processed in parallel. Cross-sections through the resulting data are extracted for analysis.

III. Calibration Load Uncertainties

Simulation begins with the determination of fundamental uncertainties such as, for example, may be assigned to the applied masses and dimensions of a calibration body. These are then used to determine the uncertainty of each applied calibration load or moment. If the calibration load plan has been shown to be adequate for determining the calibration model (DOE), then it is equally suitable for the generation of a model of the calibration load uncertainties. The calibration system uncertainty can therefore be described by a CSLu model. The CSLu model can then be used to predict the hypothetical loading uncertainty for any applied load in the calibration space. Figure 3 shows the uncertainty of each applied NF and SF load of a particular load plan in a particular calibration system. Figure 4 shows the predicted load uncertainty for an 83%FS roll-polar that was generated using a model derived from the data in Fig. 3.

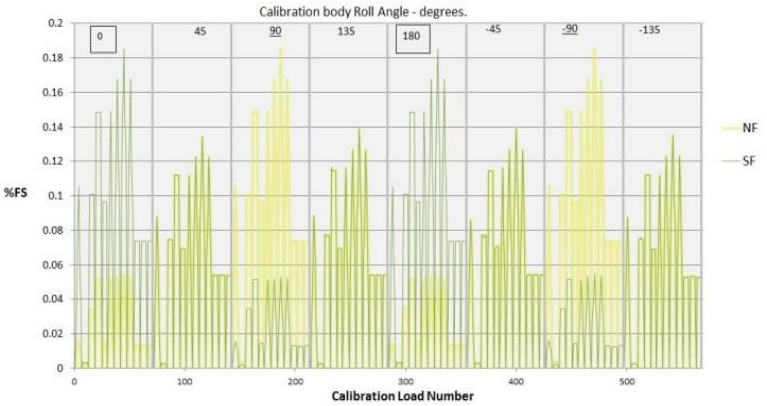

Figure 3. Uncertainties for NF and SF calibration loads

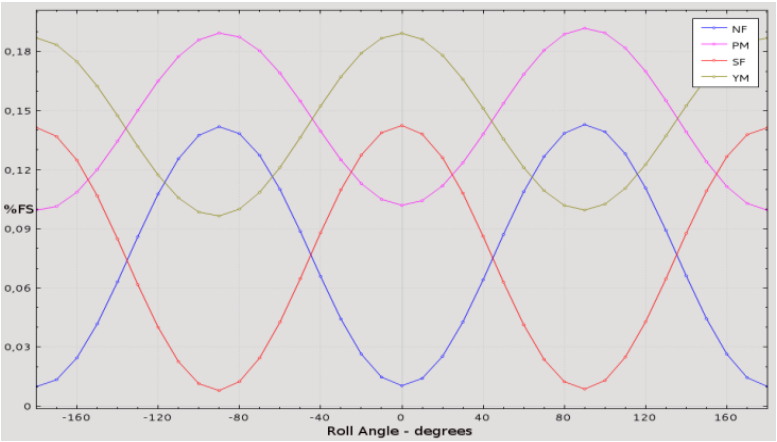

Figure 4. Roll Polar Applied-Load uncertainties at 83% load.

By applying a gravitational load to the balance, and then rotating the balance through 360 degrees, a sinusoidal load on each of the four main components, NF, PM, SF and YM can be obtained both numerically *and* experimentally. Examination of the variation of uncertainty with roll angle is a useful way of examining calibration system loading uncertainty. It additionally provides an approach to the generation and analysis of experimental data for verification of DSMC data.

Some observations from Fig. 3, are given below:

i. It can be observed that at 0 and 180 degrees roll angles, the SF load displays a greater uncertainty, (even though it is not loaded), than the applied NF load.
ii. The opposite is true at the positive- and negative-90 degree roll angles where the largest uncertainty occurs in the unloaded NF component.
iii. At the +/-45 degree and +/-135 degree angles the uncertainties are the same for the two components.
iv. These observations can also be made in Fig. 4.

The source of this unexpected result is attributable to the uncertainty in roll angle. The NF load uncertainty is a function of the the magnetude of the applied load and it's uncertainty, and the cosine of the roll-angle uncertainty,

whilst the SF uncertainty is a function of the magnetude of the applied load and it's uncertainty, and the sine of the roll-angle uncertainty. The roll-angle uncertainty, therefore, results in the major source of uncertainty of a component being that which arises from a loaded orthogonal component. The roll-angle uncertainty required to prevent this orthogonal feed-through of uncertainty can be determined, and the transition can be demonstrated on a series of curves such as those in Fig. 4.

IV. Separation of Uncertainties

A wind tunnel test generally uses a single, fixed, calibration model. Ninety five percent of the data predicted by this model is expected to be within the statistical prediction intervals. However, this is true only in the same system and under the same conditions as that in which the calibration was performed. The information required when using a balance in a wind tunnel must relate to a different system, a new installation, and data which is acquired by a different data acquisition system. If the new installation is not *exactly* the same the calibration set-up, then the prediction intervals will not be valid. The statistical prediction intervals take into account all calibration system errors as estimated from the scatter of data about a chosen regression model.

The various uncertainties that contribute to the overall balance uncertainty cannot be separated statistically. With MCS, separation of contributions to the total uncertainty can be achieved. For example, if calibration-system signal uncertainty is set to zero, the MCS simulation can be used to generate balance load-prediction uncertainties which stem from load application and regression model errors only. Similarly, the uncertainties in applied calibration loads can be set to zero. The resulting uncertainty estimates contain only the combination of the effects of signal noise and calibration-model errors. Another alternative is possible; the mean calibration model produced by MCS can be used

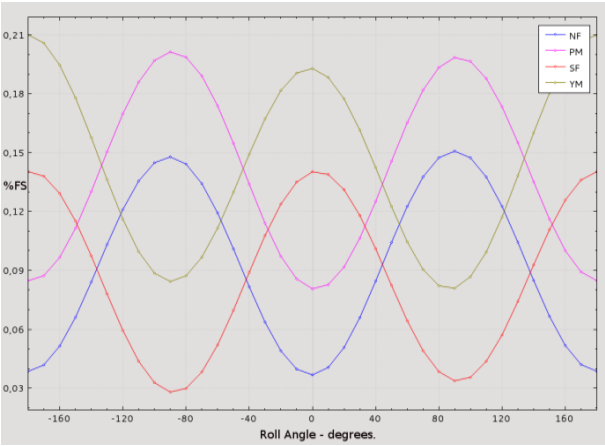

Figure 5. Model Uncertainty.

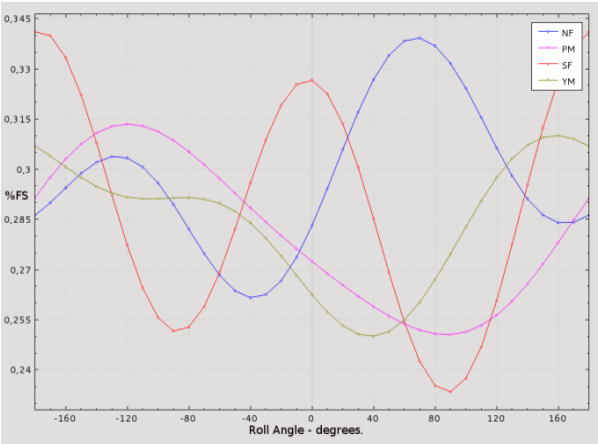

Figure 6. Total Propagated Error.

in combination with simulated signal noise. The resulting spread in generated loads is a reflection of the propagation of signal error through the model (PEs). This latter option is clearly useful in predicting the installed balance noise level in terms of load. This is both useful during installation and system evaluation.

Further work is required with respect to the separation of the various forms of uncertainty and their combination under different circumstances. At present an "upper bound" on accuracy is generated by combining the effect of the uncertainty of the model with propagated signal error. This is evaluated at a load level equal to the balance design load. For historical reasons this is referred to as the Total Propagated Error (TPE), or more recently, the inherent balance accuracy limit. The TPE is taken to be a conservative estimate of the upper bound of uncertainty/accuracy for a perfectly installed balance.

Figure 5 shows the calibration model uncertainty for NF, PM, SF and YM for a roll-polar at 83% load. Figure 6 shows the inherent balance accuracy limits (Total Propagated Error), for the same polar. The amplification in the total uncertainty due to the propagation of signal noise, through a model with uncertain coefficients, is clearly significant.

V. Uncertainty Model Limitations

In the case of the CSLu model, uncertainties are computed at calibration points and a model is fitted. In the case of calibration-model uncertainty and TPE, however, off-calibration points are specifically required. To compute models for these cases, a large number of random balance loads are simulated. Uncertainty data for these loads are then computed. Typical data is shown in Fig. 7. The data is then regressed to obtain models which can be used to generate uncertainty data at any desired load-level or combination of loads.

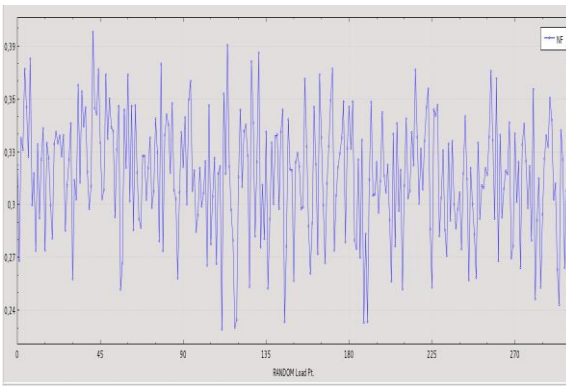

Figure 7. Typical TPE (NF) values for random off-calibration loads.

Because of the random nature of the data used to generate uncertainty models requiring off-calibration evaluations, the model fit will not be very good[6]. The distortion seen in the polar plot of Fig. 6 is evidence of this. However, the MCS software supplies a re-generation function for the random data and model, and the effect can be investigated. In general, although the shape of curves such as presented in Fig. 6, will be affected, the minimum, maximum and average values are acceptably repeatable. It is these sources of internal DSMC modeling error that result in anomolies such as seen in Fig. 9 where the TPE+Calibration-loading curve drops below the TPE curve. The use of simple linear uncertainty models instead of second order models may improve this. Further work is nevertheless required to improve these models.

VI. Situation Dependent Uncertainty

When examining loads reported by a balance, the expected uncertainty limits need to be known. The magnitudes

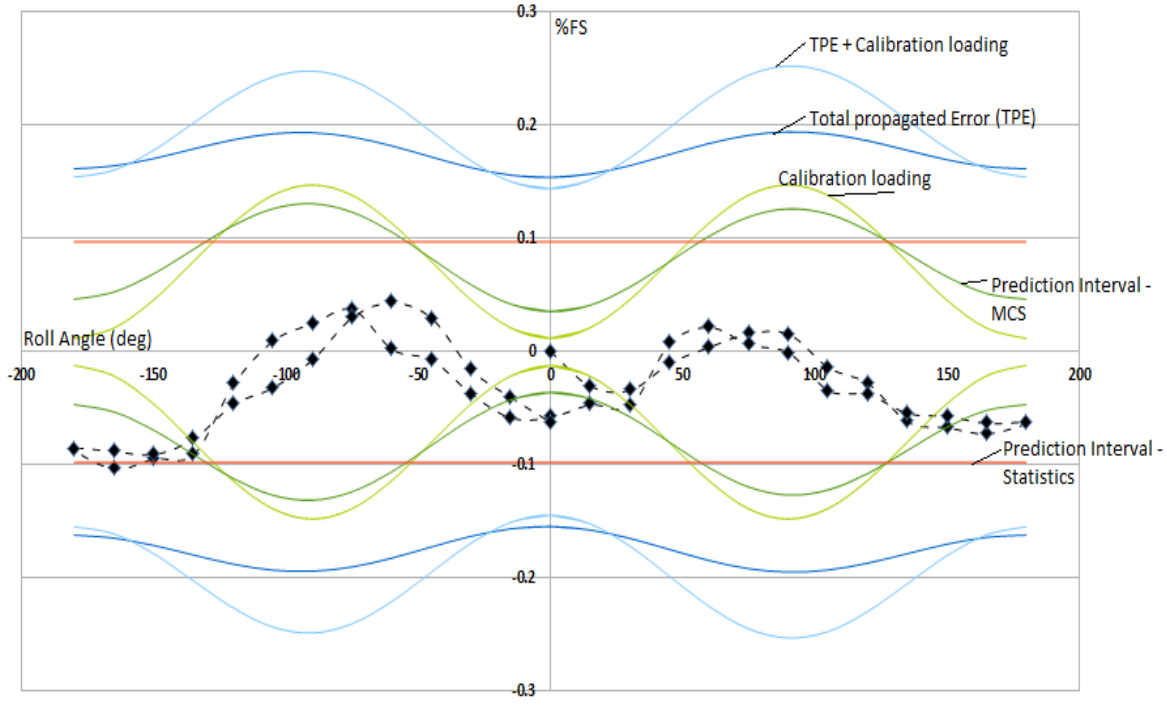

Figure 9. Various uncertainty and prediction bands plotted on actual verification data (errors) for NF. *(14mmHARMS-HA1 balance).*

of these limits are not only dependent on the magnitude and combination of applied loads, but are also dependent on the situation in which they are obtained. For example, if only the balance and its calibration model are being evaluated immediately after a calibration, the prediction intervals are suitable. The prediction intervals can also be used as an indicator of the "closeness" of an installation to the calibration setup. When post-calibration evaluations are done immediately after a calibration, signal noise can be considered small because of the static nature of the calibration process. Filtering and averaging can be used to obtain low signal noise levels. The effect of the propagated signal error can then be expected to be small. In Fig. 9 errors in the balance-reported loads (NF), from a balance are plotted together with four limits which are currently being evaluated as acceptance and/or evaluation criteria.

In the case of balance re-installation in the calibration system, additional uncertainties relating to installation need to be accounted for. Installation in a wind tunnel prior to a test requires that errors such as installation roll misalignment, pitch misalignment, as well as any additional roll or pitch measurement uncertainties are included. Some of the initial set-up errors such as roll- and pitch-misalignment can be identified, quantified and minimised through the use of roll-polar-based verification loads[8]. Peak uncertainty values in the region 0.6%FS for a fully-loaded roll-polar have been observed for primary components when all contributions are considered. This large value is an indication that the added uncertainty resulting from installation in a new system is possibly *the* major contributor to test data static force uncertainty.

VII. Data Presentation

The range of possible situations for which data can be generated by DSMC is large. Ultimately, however, the test engineer needs to know how "good" a balance is, and how well it has been installed. With the realisation of the load- and situation-dependent nature of accuracy and uncertainty, provision of a useful answer becomes problematic. At present the engineer is presented with minimum, maximum and mean values of three uncertainty metrics taken from a roll polar at full balance design load. These metrics are:

1. *Inherant Prediction Interval.*
   This is useful in installation where "closeness" to the calibration system setup is being determined. It is a repeatability guide.
2. *Inherant Total Propagated Error (TPE).*
   This is an estimate of the maximum error that can be expected from loads reported by the balance.
3. *Inherant installed TPE.*
   This is the TPE with additional errors that may arise during installation.

Note that verification data are generated using the calibration body. Therefore, calibration body loading uncertainty is included in the metrics listed above. To indicate the absence of the calibration body loading uncertainty in these quantities, the word "inherant" is added to the uncertainty metric descriptor. These data can only be obtained indirectly through a knowledge of the uncertainty of the applied verification loads. These are obtained from the CSLu model.

VIII. Statistical Comparison – Prediction Intervals

Current work is focussed on correlating calibration-model-derived statistical data with equivalent data extracted from MCS simulations. Attempts at understanding these correlations have lead to some interesting and informative results. For example, consider the prediction interval as computed using Eq. (1)[10].

$$\mathrm{PI} = t_{\frac{\alpha}{2},n-(k+1)} \sqrt{\hat{\sigma}^2\left(1 + X_p\,(X'X)^{-1}X'_p\right)} \qquad (1)$$

This equation requires an estimate of the variance, $\hat{\sigma}^2$, which is assumed to be constant and is usually estimated from the back-calculated errors (BCEs), of the calibration data with respect to the fitted regression curve. Prediction interval data generated for an 83%FS polar using the BCE as the source of the estimate of $\hat{\sigma}^2$ is shown in Fig. 10. The mean value for these prediction interval data is 0.092%FS.

The CSLu model generates point-by-point variance estimates for each load. If, instead, this is used for the variance, $\hat{\sigma}^2$, in Eq. (1), a better estimate of the prediction interval is obtained. Data generated in this way is included in Fig. 10. The mean value for this curve is 0.091%FS. The difference between the BCE-based prediction interval of 0.092%, and the average value of point-by-point prediction intervals of 0.091%, is small. Larger differences have been observed. The difference is attributed primarily to the fact that the back-calculated-error is a global curve-fit parameter derived as an average over the whole calibration space. It should not be forgotten that once the balance is removed from the calibration system, these prediction intervals are no longer valid.

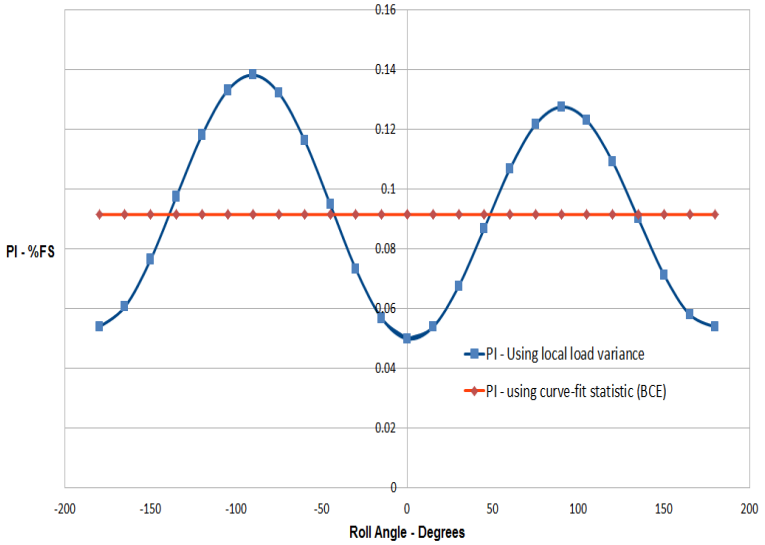

Figure 10. Positive Prediction Interval values for NF for an 83%FS roll-polar.

IX. Separation of Uncertainties

The closing statement in the previous paragraph captures the problem with respect to the estimation of *installed* balance uncertainty/accuracy. In order to achieve a reasonably representative estimate of installed balance accuracy, it is usefull to separate all contributions and to be able to selectively combine only those which are applicable under a given set of conditions. This cannot be discussed fully in a document of this length. However, an approach to the determination of the contributions to total balance uncertainty in the undisturbed calibration setup will be given here so as to provide some insight into how this separation of uncertainties is achieved.

The modeling of uncertainties, such as the calibration system loading uncertainties (CSLu), has been shown to be useful. The CSLu model can be used to generate the variation of uncertainty with roll angle for a dead-weight roll polar. Experimental data obtained from the same roll polar can then be evaluated against these simulated uncertainty data. The following discussion uses this to assist in the seperation of uncertainty contributions.

A single MCS run produces many possible calibration models (300), each of which might feasibly be generated in any repeated calibration on the same system. The mean of these models is similar to that obtained by single regression of the original calibration data which is the model which would be used in practise. These models, although they are spread about a model that itself is subject to error, and is generated from *one* set/sample of calibration data, nevertheless provide, (by their variation), usefull information about the extent to which it can be expected that any model will vary about the "true model", given the fundamental system uncertainties.

Consider the errors in experimental data shown in Fig. 11. The data shown are errors as computed by comparing balance roll-polar data with an ideal sinusoidal function[8] (the best available reference for accuracy evaluation). The plots shown in Fig. 11 are obtained using the same, fixed, set of balance data

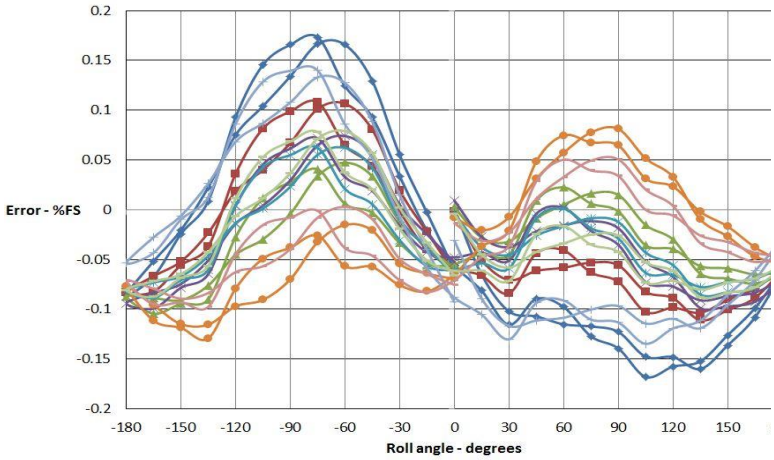

Figure 11. Balance errors for a single roll polar after processing the response data through eight feasible calibration models.

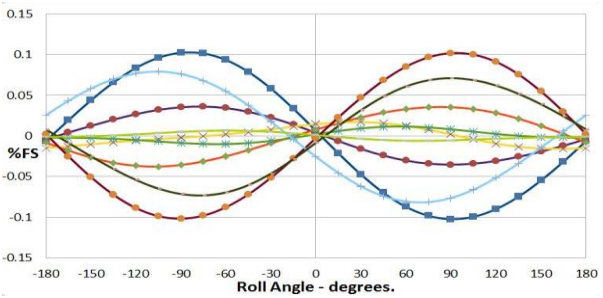

Figure 12. Underlying error sinusoids for data processed through eight feasible models.

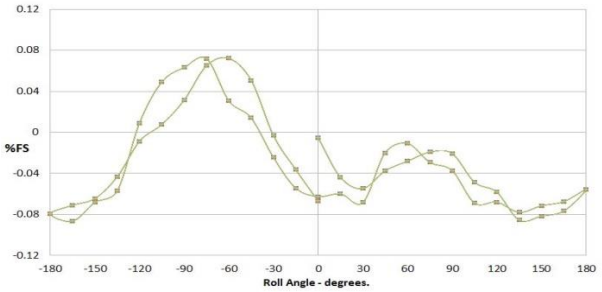

Figure 13. Errors which are independent of the calibration model.

with the errors generated in the same way for each of a series of eight feasible calibration models (eight simulation runs). The plot shown in Fig. 11 is for NF, but the same can be done for SF, PM and YM.

Figure 11 provides information regarding the variation in the error of the balance-reported load due, primarily, to variations in the calibration model. Looking beyond the larger variations in error between the models, it can be seen that there are smaller random variations that are common to the curves generated by all models. By subtracting an average of the data from each model , the common errors are separated out. The resulting plots and the removed common errors are shown in Fig. 12 and Fig. 13 respectively. This process distorts the error data since the average of the eight models will have a bias. (An infinite set of models will have no bias). The approach does however provide for effective illustration.

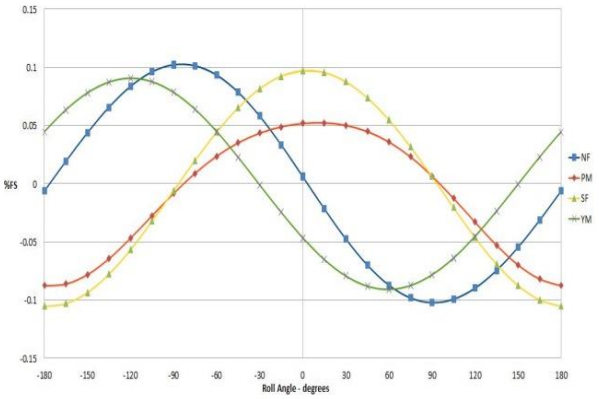

Figure 14. Model error contributions for NF, PM, SF, and YM.

The common variations shown in Fig. 13 are independent of the calibration model used. Consequently their source can be assigned to the balance signal data. The variations shown in Fig. 12 are due to variations in calibration model only. These can be seen to be sinusoidal in nature. The actual error-free magnitude of the applied NF varies cosinusoidally with roll angle. Since the errors are obtained by comparison with an ideal cosine function[8], sinusoidal variation in error implies that this error can be expressed as a small phase shift (difference in roll angle), between the ideal cosinusoidal loads and those reported by the balance. The error data for NF, PM, SF and YM are shown in Fig. 14 for one sample calibration model. These curves suggest that the phase shift might be a constant value for the four components. However, if the data is regressed[8] such that the phase shift angle is extracted, it can be seen that this is not the case. Phase shift data for a particular calibration model at this load level are given in Table 1. These differing values for phase angle are not unexpected because each component is regressed independently. Each component will therefore have it's own unique error characteristics.

Since the polar data was aquired soon after a calibration (without disturbing the system), it must be concluded that the sinusoidal portion of the error must exist in the calibration model(s). This, implies that the

Table 1. Errors as phase angle.

Component	Phase Shift (deg)
NF	-0.03
PM	0.04
SF	0.04
YM	0.01

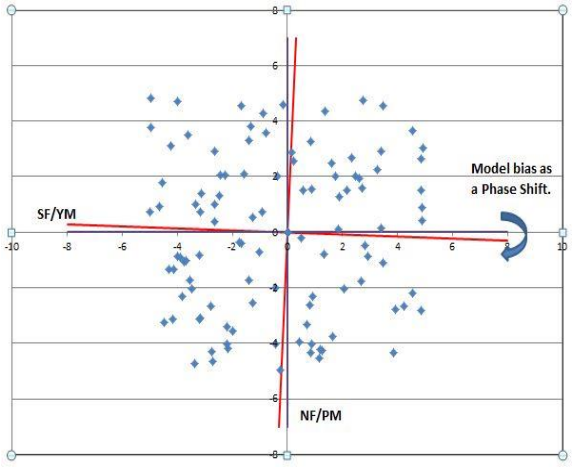

Figure 15. Illustration of Calibration Model Bias expressed as a phase shift.

local calibration model errror can be expressed in terms of a roll angle bias, which can be evaluated and modeled after calibration. The expression of balance modeling error as a phase shift angle is illustrated in Fig. 15.

X. Uncertainty Accounting

If the $2\sigma^*$ (2 standard deviations), value of 0.12% for the roll-polar error data shown in Fig. 11 is used to describe the total error for the polar, and a 2σ value of 0.072%, taken from the data in Fig. 12, is used to describe the model error, there is a difference between the two of 0.096%, which must be attributed to a combination of loading error, signal error, PEs, hysteresis and thermal drift (TMISC – total miscellaneous contribution). (A 2σ value taken from Fig. 13 is 0.097%.)

$$\text{TMISC} = \text{Total Uncertainty} - \text{Model Uncertainty}$$

$$0.096 = \sqrt{0.12^2 - 0.072^2}$$

An indication that these are reasonable estimates is obtained by comparison with predictions from the CSLu model discussed in paragraph III. A mean value of the CSLu model over the 360 degree roll polar is expected to be be similar (but smaller), than the value of 0.096% extracted from the roll polar data. The average value obtained from the CSLu model is 0.076%. A further breakdown can now be attempted. If this is subtracted from 0.096% the difference can be assigned to the remaining items listed under miscellaneous contributions viz, PEs, hysteresis and thermal drift. This is estimated to be 0.059%.

The loading error can also be estimated from the polar data. The loading error shown in Fig. 13 can be seen to be relatively repeatable at each roll angle, irrespective of the fact that a traverse was performed in both roll directions. Therefore, if the mean error at each point is assigned to loading error and and a 2σ value (0.09%) is subracted from the data, the remaining data should be a reasonable estimate of unaccounted-for MISC errors such as PEs, hysteresis and thermal drift. The mean loading error and the extracted additional errors are shown in Fig. 16 and Fig. 17 respectively. A 2σ value for MISC computed from the data in Fig. 17 is 0.048%. This is a larger than the 0.059% calculated using the CSLu model in the previous paragraph primarily due to the difference in loading error estimates.

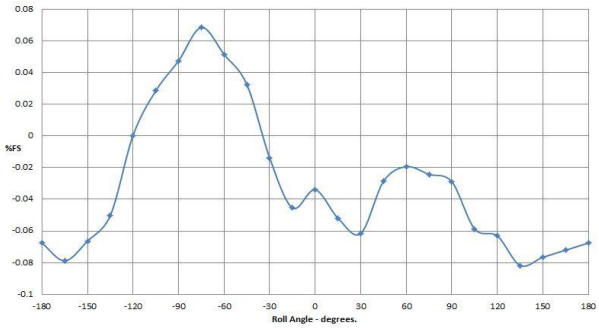

Figure 16. Mean error assigned to Calibration body loading error

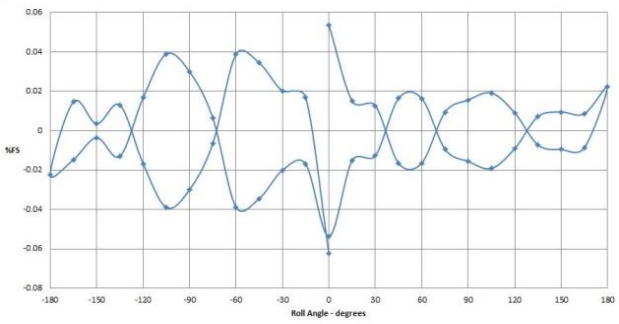

Figure 17. Baseline balance uncertainty (MISC)

The uncertainty accounting for the polar is summarised in Table 2 and Table 3. The simplified approach to uncertainty accounting described here is intended primarily as an illustration of the methedology but still raises some questions. One such question is the relatively small value of 0.091% for the prediction intervals, quoted in paragraph VIII, when compared to the total error of 0.12% given in Table 2.

Notwithstanding the fact that the value of 0.12% is obtained from data of a single polar, the polar contains 49 off-calibration loads. It is reasonable to expect the overall uncertainty to lie within the prediction intervals. Firstly the prediction value can be varified by DSMC. By setting the (propagated) signal variance to zero, an uncertainty value for the calibration model (PEm) was obtained. Twelve simulations were performed to ensure consistency of

* The 2σ value used here is a tool to estimate the order-of-magnitude of effects. It has no statistical significance since the data is not Gaussian.

results. The average model uncertainty for an 83% roll-polar was found to be 0.0909% with a standard deviation of 0.0027%. This is close to the statistically determined value of 0.092% and the single MCS value of 0.091 shown in Fig 10. This uncertainty includes loading errors and signal errors only insofar as they affect the uncertainty of the generated model. It appears, therefore, that prediction intervals are primarily an estimate of *model* uncertainty. The roll polar total uncertainty data of 0.12 given in Table 2 contains model uncertainty as well as propagated signal

Table 2. Separation of model error from total polar error.

	Uncertainty contribution %FS	Data Source	Note
Total	0.120	Polar data	Taken from 49 off-calibration data points using a sinusoidal reference[8].
Model	0.072	Polar data	Obtained from polar data after extracting errors common to all (8) models.
TMISC	0.096	Polar data (Total minus Model)	Total Miscellaneous:- Loading, Propagated Error (signal), thermal, hysteresis etc.
TMISC	0.097	Polar data (Figure 13.)	

error combined with hysteresis and thermal drift.

If, then, the value of 0.091% is the average value for the polar prediction interval, and this is the model uncertainty, what then does the 2σ taken from Fig. 12 represent? The model uncertainty value of 0.072%, was estimated from a relatively small sample of eight feasible models. This interval of ±0.072% falls, quite rightly, within the actual prediction interval of +/-0.091%, and one might accept this to be a valid estimate for the sample. However, the model uncertainty value of 0.072% is obtained using models, each of which is a *mean* model taken from a sample size of 300 calibrations (one simulation). The value is therefore more correctly a crude 2σ estimate of the standard error of the mean for the model (notwithstanding the invalidity of the statistical 2σ value).

In the foregoing discussions, three methods have been used estimate the prediction intervals and one to estimate a 2σ value for the model standard error. This data is summarised in Table 4.

Table 3. Separation of TMISC uncertainty into Loading and MISC uncertainties.

	Uncertainty %FS	Source	Note
TMISC	0.097	Polar data (Fig.13.)	Miscelaneous: Loading, Propagated Error (signal), thermal, hysteresis etc.
Loading (1)	0.076	CSLu	Loading error from simulation model.
Loading (2)	0.090	Polar data (Fig 16)	Loading error estimated from Polar data.
MISC (1)	0.059	Polar data minus CSLu	Estimated from TMISC minus loading error estimate from DSMC.
MISC (2)	0.048	Polar data (Fig 17)	Estimated from TMISC minus loading error estimate from polar data.

Table 4. Comparison of calibration model statistics using different methods.

Statistic	Value (%FS)	Tolerance	Method
Prediction Interval	0.092	-	Eqn 1 - Variance from BCE (ANOVA)
Prediction Interval	0.091	-	Eqn 1 - Variance from CSU (Partial DSMC)
Prediction Interval	0.091	+-0.003	(Pure) DSMC (300 x 12 models)
Standard Error (2σ)	0.072	-	DSMC (8 mean models)

XI. Operational Balance Accuracy

During wind tunnel testing there is no uncertainty attributable to applied loading. Therefore, loading uncertainty need not be included in the total uncertainty model. Also, if the model error can be expressed as a roll bias, it can also be neglected, minimised or at least quantified by performing dead-weight roll polars. The baseline inherent balance uncertainty will then be the MISC uncertainty (given in Table 2 as being between 0.059 and 0.048 percent of full scale for that particular load level). To this must then be added uncertainties arising from increased thermal stress, installation roll and pitch bias errors and propagated signal error, particularly if the signal noise level is significantly different from that in the calibration system.

The example used in this paper is included for purposes of providing some insight into a conceptually complex approach to uncertainty analysis. In practise, the addition or subtraction of various contributions to the final operational uncertainty estimates is done in terms of complete uncertainty models. The result is a direct computation model which can be used to generate point- specific balance uncertainty data during a wind tunnel test. Polar-specific data is only required to be generated during balance uncertainty evaluation or installation.

XII. Conclusion

The high speed version of the MCS system has only recently become functional. It will take time to fully understand balance uncertainty in a vastly variable system. What has become clear, however, is that the MCS system has moved balance data evaluation entirely into the realm of uncertainty, and by so doing has provided an effective microscope which has proven to be an effective research platform and quality assurance tool. The use of dead-weight roll polars to analyse a balance, investigate uncertainty, and to perform improved installations has also proved valuable. The work to date has yielded positive results. Development of the system has led to numerous improvements which are best illustrated by an improvement in calibration data quality being achieved in a reduced amount of time. The provision of comprehensive accuracy data for an installed balance has not yet been achieved, not least of all because of the omitted thermal contributions to uncertainty.

References

Proceedings

[1]Mark E. Kammeyer and Mathew L. Rueger. "Estimation of the Uncertainty in Internal Balance Calibration Through Comprehensive Error Propagation." Paper presented at 26th AIAA Aerodynamic Measurement Technology and Ground Testing Conference. Seattle, Washington : s.n., AIAA 2008-4029, June 2008.

[2]Bidgood, P.M., "A Parameter for the Selection of an Optimum Balance Calibration Model by Monte Carlo Simulation." Eighth South African Conference on Computational and Applied Mechanics, Johannesburg, South Africa, 3–5 September 2012, © SACAM, eISBN:

[3]Bidgood P.M., "Comparison of Second and Third Order Wind Tunnel Balance Calibration models using Monte Carlo to Propagate Elemental Errors from Calibration to Installation." Paper presented at 51st AIAA Aerospace Sciences Meeting including the New Horizons Forum and Aerospace Exposition : Grapevine, Texas : s.n., AIAA 2013-0544, eISBN: 978-1-6, June 2013.

[4]Bidgood P.M., "On the speed-up of balance calibration matrix generation and uncertainty analysis by MCS on a GPU platform.," Paper presented at 9th International Symposium on Strain-Gauge balances, Seattle, Washington. May 2014.

[5]Ewald, Bernd. "The Uncertainty of Internal Wind Tuinnel Balances. Definition and Verification." Darmstadt,Germany : 3rd International Symposium on Strain-Gauge Balances., 13-16 May,2002.

[6]N.Ulbrich, "Assessment of the Uniqueness of Wind Tunnel Strain-Gage Balance Load Predictions." 32nd AIAA Aerodynamic Measurement Technology and Ground Testing Conference. Washington, D.C. AIAA 2016-41157, June 2016.

[7]P.M.Bidgood, C.M.Johnston. "Uncertainty project." *Report.* Pretoria,SA : CSIR, April,2005. DEF 2005/033.

[8]Burger A. ” Using Roll-Polars for Balance Error Generation in Installation and Uncertainty Estimation.”. Paper presented at 55st AIAA Aerospace Sciences Meeting. Grapevine, Texas : AIAA (Not available at time of printing) 9-13, January 2017.

[9]T.Volden, N.Ulbrich. "Development of a New Software Tool for Balance Calibration Analysis." Paper presented at 25th AIAA Aerodynamic Measurement Technology and Ground Testing Conference. San Francisco,California : s.n., AIAA 2006-3434, June 2006.

Books

[10]Samprit Chatterjee and Ali S Hadi., "Regression Analysis by Example." 4th Edition, John Wiley & Sons, Inc., 2006. ISBN:0-471-74696-7

[11]Coleman, H.W. and steele, W.G. "Experimentation and Uncertainty Analysis for Engineers." New York, NY : John Wiley & Sons, Inc., 1989.

Reports, Theses, and Individual Papers

[11]AIAA. Recommended Practice. "Calibration and Use of Internal Strain-Gage Balances with Application to Wind Tunnel testing." s.l. : American Institute of Aeronautics and Astronautics , 2003. Vol. 1. ISBN 1-56347-646-0.

[12]AIAA. Assessment of Wind Tunnel Data Uncertainty. 1995. S-071-1995.

[13]P.M.Bidgood, C.M.Johnston. "Uncertainty project." *Report.* Pretoria,SA : CSIR, April,2005. DEF 2005/033.

[14]Bidgood P.M., “Internal Balance Calibration and Uncertainty Estimation using Monte Carlo Simulation.” D.Ing Thesis, Faculty of Engineering and the Built Environment, University of Johannesburg, South Africa, June 2013.

[16]David M Cahill. "Balance Calibration Uncertainty - Introduction to discussion on standardisation." Presentation. Zwolle, The netherlands : 6th International Symposium on Strain-Gauge balances, 5-8 May,2006.

[17]N.Ulbrich, T.Volden. "Development of a New Strain-Gage Balance Calibration Analysis Capability at NASA Ames Research Center." Zwolle,The Netherlands : 6th International Symposium on Strain-Gage Balances, 2008.

[18]T.Volden, N.Ulbrich. "Regression Model Term Selection for the Analysis of Strain–Gage Balance Calibration Data." Williamsburg, Virginia : 7th International Symposium on Strain-Gauge balances, 11-13 May,2010.

[19]Hufnagel, Klaus. "Common definition of Balance Accuracy and Uncertainty." Williamsburg, Virginia : 7th International Symposium on Strain-Gauge Balances, 11-13 May,2010.

[20]Bidgood.P.M., "Development of the Ø14mm-HARMS-3t Balance.", 7th International Symposium on Strain-Gauge Balances, Williamsburg, Virginia, May,2010

[20]Bidgood.P.M., "Balance Matrix Generation by Monte Carlo Simulation." 8th International Symposium on Strain-Gauge Balances, Lucern, Switzerland, May, 2012